Electron-paramagnetic resonance detection with software time locking

Giovanni Aloisi,[1,a)] Matteo Mannini,[1] Andrea Caneschi,[1] David Dolci,[1,2] and Marcello Carlà[2]

[1]*Department of Chemistry and INSTM Research Unit, University of Florence, Via della Lastruccia 3, 50019 Sesto Fiorentino (FI), Italy*

[2]*Department of Physics, University of Florence, Via G. Sansone 1, 50019 Sesto Fiorentino (FI), Italy*

(Received 2 September 2013; accepted 27 January 2014; published online 20 February 2014)

A setup for electron paramagnetic resonance with narrow band digital detection is described. A low frequency reference tone is added to the radio frequency signal. This reference signal, after digital detection, is used to lock the resonance signal, even in the absence of hardware time locking among the radio frequency generator, the conversion local oscillators, and the sampling stage. Results obtained with 2,2-Diphenyl-1-Pycryl-Hydrazil are presented and discussed. © *2014 AIP Publishing LLC*. [http://dx.doi.org/10.1063/1.4865133]

I. INTRODUCTION

Electron Paramagnetic Resonance (EPR) is a spectroscopic technique based on the adsorption of electromagnetic waves in the microwave region by electronic spin states immersed in a magnetic field and has found numerous applications in chemistry, physics, and medicine.

Attempts to develop microscopic EPR techniques, to allow a local analysis of the spin states at the micro- and (possibly) at the nano-scale, are dealing with smaller and smaller sample quantities[1] and require to increase the sensitivity towards low level signals.

Actually the signal expected in Electron Spin Noise - Scanning Tunneling Microscopy (ESN-STM)[2–4] has been estimated to be of the order of −130 dBm.[5]

The inductive detection of EPR and Nuclear Magnetic Resonance (NMR) signals with micro-coils is a subject of intensive research,[6–9] focused on the development of both smaller probes and more efficient detection schemes.

Recently, non-miniaturized single loop coils simply connected to a coaxial cable have been shown to be very convenient probes allowing complex EPR measurements with a simple experimental set-up over a wide frequency band and in the temperature range from a few *K* to room temperature.[10,11] Operating with a probe that is not tuned to a specific frequency yields a noisier signal because of the absence of the filtering action of the tuned circuit, but can be worthy of with geometries with an unstable impedance as, for example, STM probes.[12] However, the absence of a narrow filtering in the probe assembly can be compensated almost entirely with a narrow band detection procedure, which is now easily implemented with digital detection.[13,14] In order to test this approach, we have studied the detection of the signal reflected by a single loop coil that surrounds an EPR sample immersed in a magnetic field. This constitutes a handy probe to work with, suitable for instrument setup and calibration.

Detection of the small perturbation in the electromagnetic field induced by the presence of EPR in a sample usually requires the use of a lock-in technique; normally, this is implemented applying a small modulation to the sample magnetizing field and synchronously detecting the resulting Amplitude Modulation (AM) of the Radio Frequency (RF) carrier coupled to the sample.[15]

Synchronous detection can be achieved using a lock-in amplifier to process the low frequency signal obtained by AM detection of the modulated RF carrier, e.g., using a crystal detector.[10] Alternatively, single side band (SSB) detection can be used, processing only the upper or lower modulation sideband at frequency $f_0 \pm f_m$, generated by the AM modulation of the carrier f_0 with the modulation signal f_m. The advantage of this last arrangement lays in the narrower bandwidth that can be used in the signal amplifying chain. Actually, with an AM detector, bandwidth cannot be less than $2 \cdot f_m$, where f_m is in the range from 10 to 100 kHz. With SSB detection, the bandwidth can be narrowed, ideally, to the level of the following lock-in detector bandwidth (from a fraction of to a few *Hz*), resulting in a lower noise level at the input of the lock-in detector.[14] Moreover, preventing the carrier from reaching the Analog-to-Digital Converter (ADC) greatly reduces dynamical range requirements in the signal digitization.

However, the use of SSB detection poses severe restrictions over the instrumentation setup, because of the frequency stability required in the oscillators for frequency conversions in the amplifying chain.

As discussed by Hyde,[16] different solutions are possible in the front end of an EPR spectrometer, e.g., homodyne detection, superheterodyne down-conversion and detection, and direct (sub)sampling of the microwave signal.[17,18] But independently of the solution adopted before the ADC, all frequency generators used in the spectrometer, including the ADC sampling clock if digital detection is implemented,[13] should be closely locked to a single master oscillator. Failure to comply with this requirement results, in the authors' analysis, in degraded instrument performances.[16]

This can be exemplified by considering that to measure the phase changes of the signal with respect to the RF excitation with an error of 3° (about 10^{-2} cycles) in a magnetic field scan lasting 10^3 s, a frequency drift less than 10^{-5} Hz/s is needed between the signal to be detected and the reference signal.

a)Electronic mail: aloisi@unifi.it

A complete locking is not easily implemented using general purpose readily available hardware.

In this work, we propose, as a relatively simple alternative, to replace the lock of the full oscillators chain with a software lock through a reference tone added to the carrier. The proposed technique has been implemented in a superheterodyne down-conversion EPR receiver, using a Spectrum Analyzer (SA) to down-convert the RF signal to the low frequency signal of the last Intermediate Frequency (IF). This output is acquired by a general purpose Digital Acquisition (DAQ) board.

At the core of the experimental setup, we have used a dual Direct Digital Synthesis (DDS) signal generator that yields two low frequency tones that are strictly synchronous by the very nature of the generator (alternatively, two single DDS generators can be used, but they must be locked to a common clock: phase coherence between the two tones is a requisite of the technique).

One of these tones is used to drive a couple of auxiliary coils that modulate the magnetic field applied to the sample; the other one is used to add a reference marker by applying a small level of amplitude modulation to the radio frequency signal used to excite the electron resonance. Hence, at resonance, the signal that is obtained from the sample and reaches the input of the SA contains five spectral components: the RF carrier and four sideband signals, two from each one of the modulating tones. At the IF output of the SA only the two upper sideband signals are allowed through the last IF filter, the other sideband and the carrier being removed. This signal is sent to the first of a dual channel ADC, the other being used to sample one of the original tones from the DDS. Then, a software algorithm directly performs a synchronous IQ detection.

II. EXPERIMENTAL SETUP

The measurement setup is sketched in Fig. 1. The sample is immersed in the magnetic field generated by a Varian 4005 Electromagnet and modulated by a couple of 20 turns 8 cm diameter coils (coil gap is 3.5 cm). A single turn 8 mm diameter probe coil made of silver plated 1 mm diameter copper wire surrounds the sample. The axis of the coil is perpendicular to the magnetic field.

A RF signal, with frequency f_0 in the range $300-800$ MHz and amplitude equal to 0 ± 0.4 dBm, originated by a Marconi 2019A generator, is routed to the probe coil by an Anzac H-1-4 hybrid coupler and a 12 cm segment of RG402 semi-rigid coaxial cable; the signal, reflected from the probe coil, through the same hybrid coupler reaches the HP 8563E SA, where it is amplified, filtered, down-converted to 4.8 kHz, and made available for analog to digital conversion. To reduce the background signal f_0 reflected by the coil, a second "mirror" probe and coaxial line of identical design is connected to the other hybrid coupler port. Since the hybrid junction introduces a 180° phase difference between the two paths, the two probe signals mostly cancel each other at the output port of the coupler. With 0 dBm at the input of the coupler, the output is about -50 dBm over the whole frequency range. The EPR signal, being generated only in the sample branch, does not suffer such a cancellation. The hybrid coupler insertion loss is about 10 dB; hence the signal cancellation due to the two matched probes arrangement is about 40 dB.

In the usual 3 ports "circulator" configuration,[8,19] where the signal from the port opposite to the probe is nulled by a matching resistor, an output power of -10 dBm was measured.

It should be noted that if the coil is tuned and impedance matched to the line adding a series and a parallel capacitor, the reflection of the carrier at the resonance frequency can be nulled to zero anyhow and the 3 ports circulator configuration is the best choice, at the expense of missing broad band operation.

The dual DDS synthesizer HP3326A generates two tones. The first one, the field modulation signal, with frequency $f_m = 16$ kHz, is sent through a 100 W, 50 kHz power amplifier (Prism Audio MTK100PS) to the two modulating coils, providing a field modulation of 100 μT.

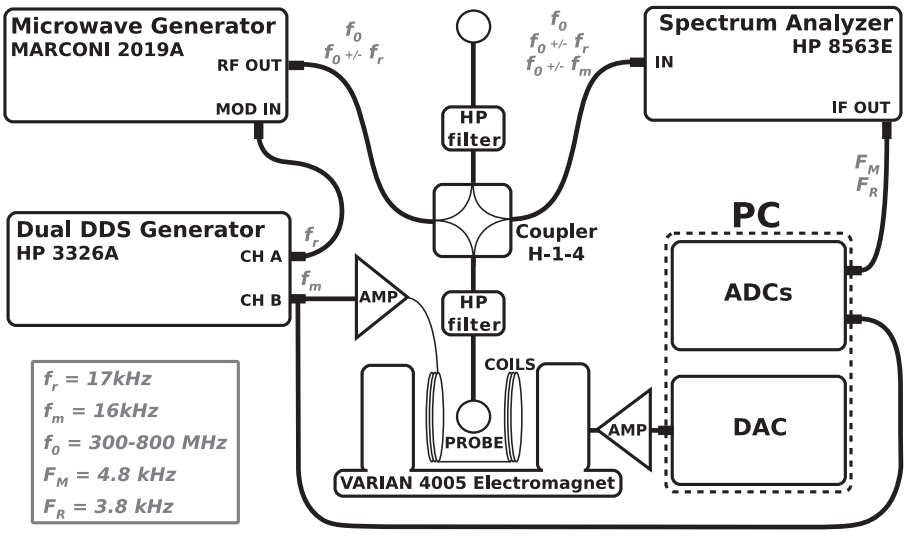

FIG. 1. Schematic of the single loop spectrometer. Details are given in the text.

The second tone from the DDS generator, i.e., the reference marker, with frequency $f_r = 17$ kHz, is applied to the amplitude modulation input of the RF generator. Levels are adjusted in order to give side band signals 60 dB lower than the carrier. In this way, the signal is strong enough to be easily detected after the digital acquisition. The five components in the RF signal at the input of the spectrum analyzer at frequencies $f_0, f_0 \pm f_r, f_0 \pm f_m$ have amplitudes respectively -50 dBm, -110 dBm, and -105 dBm at the resonance peak. Other components that appear at frequencies $f_0 \pm f_r \pm f_m$ have negligible amplitudes.

The bandwidth of the IF filter of the SA is set to 500 Hz and peaked to the $f_0 + f_m$ EPR signal component. This bandwidth is the minimum available value for the IF SA filter; a final narrower bandwidth for the EPR signals is obtained at a later stage during the digital IQ detection. Even if the $f_0 + f_r$ reference marker component remains out of the filter pass-band and is reduced in amplitude by 30 dB it is still easily detectable at the SA output. Carrier f_0 and lower sideband signals are instead efficiently rejected to a negligible intensity.

The output at the last IF of the SA contains the EPR signal at the nominal frequency $F_M = 4.8$ kHz and the reference signal at an F_R frequency 1 kHz lower (there is a side band reversal in the SA down-conversion chain). This signal is digitized at a 100 kHz sampling rate using a National Instrument NI6221 DAQ board in a PC under the control of the SPM2 software package. This open source package, operating in a Linux environment, has been originally developed for real time control of the feedback of a scanning microscope.[20–22]

The second channel of the ADC is used to directly sample the f_m signal. Acquired data are stored to disk for off-line processing. The software is responsible also for scanning the magnetic field via one of the Digital to Analog Converters of the DAQ board, that drives the Varian 2901 power supply.

It has been observed that even with a small deviation from orthogonality between the modulation field and the coil axis the 16 kHz magnetic field modulation can induce an emf in the probe coil. If this signal reaches the hybrid coupler it can modulate the RF leakage between input and output port. This effect generates a signal indistinguishable from the true EPR resonance and can be a source of measurement errors especially in case of very low EPR signals. To avoid this, a couple of high-pass filters (Mini Circuits SHP-25) with corner frequency 25 MHz has been introduced to block the transmission of low frequency components from the probe to the hybrid coupler.

The magnetic field has been monitored with a Honeywell Hall probe mod. SS495A with a 5% absolute accuracy, a 0.5% reproducibility, and a sensitivity of 62.5 V/T.

The samples used in the measurements were composed by 2,2-Diphenyl-1-Pycryl-Hydrazil (DPPH) by Sigma-Aldrich, used as received, and were contained in a standard plastic 0.5 mL micro-centrifuge vial (7.6 mm o.d.), placed at the center of the probe coil. The vial containing the DPPH sample has been weighted before and after filling with the sample with a Mettler Toledo MX5 microbalance with $1\mu g$ resolution. Error on the DPPH weight due to the normal vial handling and environmental humidity changes has been estimated to be less than 30 μg.

III. DATA ACQUISITION AND PROCESSING

A typical spectrum is taken scanning over 120 to 400 different magnetic field values in an interval 3.6 to 9 mT wide and acquiring a single set of 10^5 samples for each field value, for a total of 4×10^7 samples in 400 s. To maintain the signal phase coherence, it is necessary to acquire each sample set in a continuous data stream, with no interruption or sample loss. This is achieved using the SPM2 package to drive the signal acquisition and generation by the DAQ board, under the control of a Labview[23] program.

Each dataset at constant magnetic field intensity is split into N subsets, the $I - Q$ (in-phase and quadrature) components of the EPR signal are determined for each of the subsets, and an average is made over the N results obtained. The optimal value for N has been determined experimentally as discussed later.

The elaboration of the data in each subset proceeds as follows.

First, the frequency F_R and phase Φ_R of the reference signal is calculated using the LabView "single tone extract" function,[23] constraining the search in a 100 Hz wide window, centered at the 3.8 kHz nominal value. Then the frequency F_M, the sought frequency of the synchronous detection signal, is recovered.

Considering that the frequencies F_R and F_M are the result of the frequency conversion of respectively f_r and f_m and that during superheterodyne conversion the same frequencies are added or subtracted to both f_r and f_m, we may safely assume that the difference $F_R - F_M$ is the same as the original difference $f_m - f_r$ set by the DDS generator, the sign reversal being due to a sideband reversal in one of the IF conversions.

This frequency difference in the acquired data is not exactly 1 kHz because in our setup the sampling clock of the DAQ board is not locked to the DDS generator clock. This can be corrected by sampling the 16 kHz signal with the second ADC channel and determining with the same "single tone extract" function the dominant tone f'_m in the acquired signal.

Now we may define the difference between F_R and F_M to be $1\ \text{kHz} \cdot f'_m/16\ \text{kHz}$.

Once that F_M has been determined we may calculate the phase of the detection signal Φ_M as follows: we assume an arbitrary phase difference between the reference and the detection signals at the beginning of the first data subset and calculate the number of cycles and fraction of a cycle contained in the subset sequence time length for both the two frequencies F_R and F_M. By taking the difference between the two numbers we obtain the increment in the phase difference between the two signal in the given subset; this phase difference, added to Φ_R, gives Φ_M.

The value of the phase at measure start time is defined "*a posteriori*" to yield a zero of the phase at the frequency of paramagnetic resonance.

After the exact values of frequency and phase of the synchronous reference signal are known, the sin() and cos() values are calculated for the time of each value in the subset;

from the scalar products of these two vectors with the sampled data, the I and Q components for the subset are determined.

IV. RESULTS

A data acquisition of 4×10^6 samples for 120 magnetic field values has been made at a frequency of 700 MHz for a 50 mg DPPH sample and has been processed using several different data subset lengths to determine the best subset length and corresponding N value. Results are reported in Fig. 2.

With a subset of 10^3 samples, spanning a time of 10 ms, and with shorter subsets, the resonance peak becomes small and noisy, because of a poor determination of the reference frequency F_R that leads to a poor accuracy in the F_M and Φ_M values.

On the other side, if the sampling length is extended to more than 2 s (i.e., 2×10^5 samples), the shape of the peak appears degraded because of loss of phase coherence of the oscillators in the generation/conversion chain over a so long time period.

Hence, using a subset length in the wide range between these two limits it is possible to have a long enough samples vector to compute F_R and Φ_R with the required high level of accuracy, without the penalty of loss of phase coherence that occurs on longer times because of the lack of the oscillators synchronization to a common clock.

A length of 200 ms has been chosen as a good compromise and has been used in all following computations.

In Fig. 3, the spectra taken for a 50 mg DPPH sample are reported for frequencies going from 300 MHz to 800 MHz at 100 MHz intervals. For each frequency, 10^5 samples in 1 s have been acquired for 400 values of the magnetic field. Modulus is reported in the upper part of the figure, phase in the lower part.

The experimental data, both the real (I) and imaginary (Q) components, have been fitted with the derivative of the harmonic oscillator resonance curve (akin in modulus to the *lorentzian* function) using the least squares Marquardt–Levenberg algorithm available with the "gnuplot" data graphing utility.[24] Four parameters were adjusted by the fit, namely the magnetic field at the resonance peak, the peak width, the phase offset at the resonance, and the peak height.

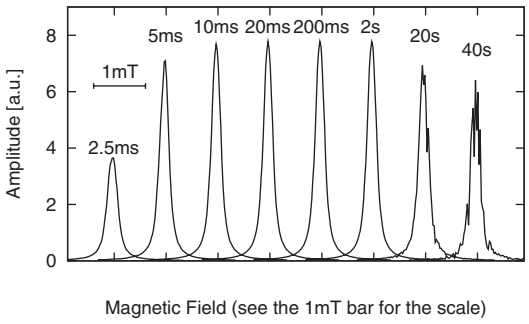

FIG. 2. EPR signals obtained with a sample of 50 mg DPPH at 700 MHz for different length values of the analysis subsets (see text). The peaks have been shifted horizontally for clarity. Time per point is 40 s.

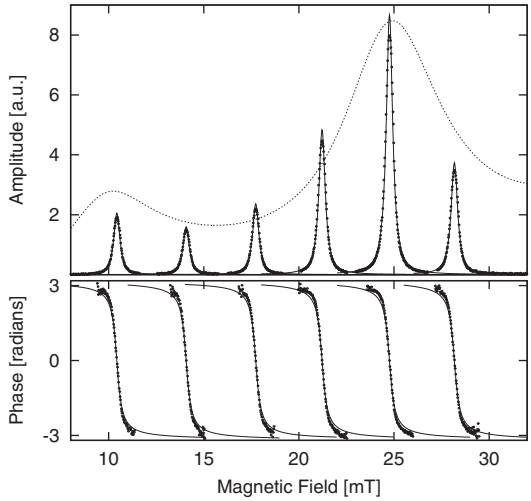

FIG. 3. EPR signals obtained with a sample of 50 mg DPPH. Frequency from 300 MHz to 800 MHz in 100 MHz steps. Dots: experimental points; solid lines: analytical function with parameters from the fit; and dotted line: calculated sensitivity (see the Appendix). Upper plot: modulus; lower plot: phase.

Results of the fit are reported as solid lines in the figure. The SNR of the peaks, evaluated as the ratio of the peak height to the RMS noise on the baselinen is about 1000 for the highest peak.

The dependence of the peak heights with frequency is not monotonic, as could be expected by the well-known linear relation between spin population and resonance frequency.[25] This is essentially due to the impedance mismatch at both sides of the 50 Ω rigid coaxial cable, which is connected to the frequency dependent coil impedance on one side and the 100 Ω port of the coupler on the other. These mismatches causes reflection in the coaxial cable and make the transmission of the probe signal dependent on the frequency. We have evaluated the frequency dependence of the probe sensitivity as explained in the Appendix.

Thereafter, the sensitivity has been multiplied by the frequency to account for the increase of the spin population due to the so called Boltzmann factor[25] and reported in Fig. 3 (dotted line in the upper plot). A scaling factor has been introduced, to make equal the sums of the six experimental peak heights and the six computed values at the measure frequencies. It can be seen that the computed curve reproduces fairly well the frequency dependence of the peak heights.

The signal to noise ratio of the spectra in Fig. 2 is 1000 (60 dB). Since, as mentioned earlier, the EPR signal intensity is −105 dBm, it follows that the noise background of the spectra is −165 dBm.

This quantity is in agreement with the constructor's specifications for the SA, that declare a Displayed Averaged Noise Level (DANL) better than −150 dBm at 1 Hz bandwidth (our bandwidth with one second measurements is about 0.14 Hz, that accounts for 9 dB). Hence the SA noise floor is the limiting factor in the measuring system performances.

We think therefore the method has enough sensitivity for the detection of the estimated ESN-STM signals in a time compatible with scanning operations. To verify this

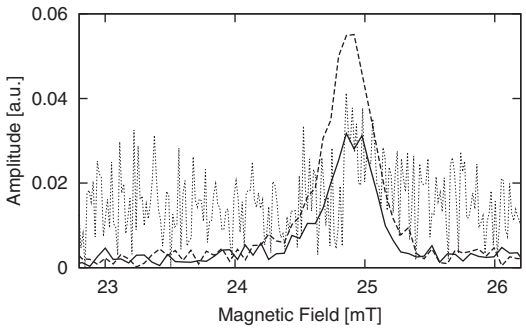

FIG. 4. EPR signals obtained with a sample of 0.2 mg of DPPH. Dotted line: 0 dBm generator power, 1 s time per point; solid line: 0 dBm generator power, 40 s per point; and dashed line: 5 dBm generator power, 40 s per point. Amplitude unit is the same as in Figures 2 and 3.

sensitivity, we determined the resonance peak for a sample of 0.2 mg (Fig. 4). With the same measure and average time used for data in Fig. 2, the peak is barely discernible over the background (dotted line), with a S/N factor of 2, in agreement with the expected proportionality between the peak height and the sample quantity. A better S/N may be obtained both by increasing the measure time, which reduces the noise background (solid line), and increasing the RF input from the generator (dashed line). Proportionality between generator power and signal amplitude shows we are below spin saturation. This is expected from the low level of the RF magnetic field intensity, estimated to be below 1 μT (at 0 dBm generator power).

ACKNOWLEDGMENTS

This work has been supported by MIUR (PRIN RECORD 20097X44S7), FP7-PEOPLE-2011-IAPP - ESNSTM - GA 286196, and "Ente Cassa di Risparmio di Firenze".

APPENDIX: EVALUATION OF THE PROBE SENSITIVITY

The instrumental sensitivity as a function of the frequency has been calculated under the following two assumptions:

(i) the interaction between the probe coil and the sample can be described as a (small) change in the coil inductance because of the presence of the paramagnetic sample, characterized by a complex magnetic permeability $\mu^*(f)$ function of the frequency;
(ii) the derivative of the inductance L of the probe with respect to $\mu^*(f)$ depends upon the frequency only through $\mu^*(f)$.

Under these assumptions, the instrumental setup sensitivity has been evaluated as $s(f) = |dS_{11}/dL|$ where S_{11} is the reflection coefficient at the junction between the coupler and the probe assembly composed by the filter, a short segment of transmission line and the single loop coil, as shown in Fig. 1.

In order to compute the dS_{11}/dL derivative, the properties of all the components of the probe assembly have been measured in the frequency range of interest using a Vector Network Analyzer Anritsu mod. MS6441A; thereafter, the $S_{11}(f)$ function has been constructed and numerically differentiated.

In the probe model, a small stray capacity (C) has been considered at the junction between the coil loop L and the line, because of the presence of a few mm of wires, and a resistance (R) has been added in series to the probe inductance to account for losses.

The values for L, C, and R could not be obtained by a direct measurement because they are significantly affected by the connection with the line; hence the line has been measured twice. The reflection coefficient S_{11}^o of the line left open was measured first and through a least squares fit on both the real and imaginary part of S_{11}^o the electrical line length and loss were obtained. Then the reflection coefficient S_{11}^p of the line terminated with the coil loop was measured. From these data and using the previous results for the transmission coaxial line, the coil parameters L, R, and C have been determined, again by least squares fit. In both cases, the residuals between experimental and model data using the fitted parameter values were of the order of -40 dB, in good agreement with the expected analyzer accuracy.

The high pass filter was analyzed measuring its S_{11}^f and S_{21}^f parameters. The value of S_{11}^f resulted to be negligibly small (of the order of -40 dB) over the whole $300 - 800$ MHz frequency range; the S_{21}^f parameter showed a practically constant insertion loss with a linearly changing phase from 300 to 800 MHz.

All these data were combined to obtain the probe impedance as seen at the junction with the coupler and from this the S_{11} reflection coefficient. The sensitivity $s(f)$ was computed by numerical differentiation $|(S_{11}(L + dL) - S_{11}(L))/dL|$ where dL is a small arbitrary complex quantity.

The single significant source of error in the probe assembly model comes from a ± 3 mm uncertainty in the length of an adapter that has been used between the N type connector of the Anritsu analyzer and the SMA connectors of the probe assembly (to be subtracted from the line length). This uncertainty has been verified to introduce on average a 4% change in the peak heights.

[1] A. Blank, E. Suhovoy, R. Halevy, L. Shtirberga, and W. Harneitb, Phys. Chem. Chem. Phys. **11**, 6689 (2009).
[2] Y. Manassen, R. J. Hamers, J. E. Demuth, and A. J. Castellano, Jr., Phys. Rev. Lett. **62**, 2531 (1989).
[3] M. Mannini, P. Messina, L. Sorace, L. Gorini, M. Fabrizioli, A. Caneschi, Y. Manassen, P. Sigalotti, P. Pittana, and D. Gatteschi, Inorg. Chim. Acta **360**, 3837 (2007).
[4] P. Krukowski, W. Olejniczac, Z. Klusek, S. Pawlowski, P. Kobierski, and M. Puchalski, Measurement **43**, 1495 (2010).
[5] P. Messina, M. Mannini, A. Caneschi, D. Gatteschi, L. Sorace, P. Sigalotti, C. Sandrin, S. Prato, P. Pittana, and Y. Manassen, J. Appl. Phys. **101**, 053916 (2007).
[6] H. Mahdjour, W. G. Clark, and K. Babershke, Rev. Sci. Instrum **57**, 1100 (1986).
[7] Y. Morita and K. Ohno, J. Magn. Reson., Ser. A **102**, 344 (1993).
[8] G. Boero, M. Bouterfas, C. Massin, F. Vincentem, P. A. Besse, R. S. Popovic, and A. Schweiger, Rev. Sci. Instrum. **74**, 4794 (2003).
[9] R. Narkowicz, D. Suter, and R. Stonies, J. Magn. Reson. **175**, 275 (2005).
[10] Z. H. Jang, B. J. Suh, M. Corti, L. Cattaneo, D. Hainy, F. Borsa, and M. Luban, Rev. Sci. Instrum. **79**, 046101 (2008); **79**, 079901 (2008).

[11]M. Corti, L. Cattaneo, M. C. Mozzati, F. Borsa, Z. H. Jang, and X. Fang, J. Appl. Phys. **109**, 07B104 (2011).
[12]U. Kemiktarak, T. Ndukum, K. C. Schwab, and K. L. Ekinci, Nature (London) **450**, 85 (2007).
[13]L. Gengying and X. Haibin, Rev. Sci. Instrum. **70**, 1511 (1999).
[14]M. P. Tseitlin, V. S. Iyudin, and O. A. Tseitlin, Appl. Magn. Reson. **35**, 569 (2009).
[15]J. S. Hyde, P. B. Sczaniecki, and W. Froncisz, J. Chem. Soc., Faraday Trans. 1 **3901**, 85 (1989).
[16]J. S. Hyde, T. G. Camenish, J. J. Ratke, R. A. Strangeway, and W. Frocisz, in *Biomedical EPR: Part B*, edited by S. S. Eaton, G. R. Eaton, and L. J. Berliner (Kluwer, New York, 2005), Chap. 7.
[17]J. S. Hyde, H. S. Mchaourab, T. G. Camenish, J. J. Ratke, R. W. Cox, and W. Froncisz, Rev. Sci. Instrum. **69**, 2622 (1998).
[18]J. Forrer, H. Schmutz, R. Tschaggelar, and A. Schweiger, J. Magn. Reson. **166**, 246 (2004).
[19]M. Alecci, S. Della Penna, A. Sotgiu, L. Testa, and I. Vannucci, Rev. Sci. Instrum. **63**, 4263 (1992).
[20]G. Aloisi, F. Bacci, M. Carlà, D. Dolci, and L. Lanzi, Rev. Sci. Instrum. **79**, 113702 (2008).
[21]G. Aloisi, F. Bacci, M. Carlà, and D. Dolci, Rev. Sci. Instrum. **81**, 073707 (2010).
[22]See http://spm.polosci.unifi.it for SPM2, open source software for real time control of a Scanning Probe Microscope.
[23]Labview 8.6, National Instrument, see http://www.ni.com.
[24]See http://www.gnuplot.info/ for gnuplot, an open source graphing utility for data visualization.
[25]*Multifrequency Electron Paramagnetic Resonance*, edited by S. K. Misra (Wiley-VCH, Winheim, Germany, 2011).